Researchers Journal of Science and Technology (REJOST)
https://rejost.com.ng

Post seismo-ionospheric perturbations linked to the Turkey earthquake of February 6, 2023 using GPS-TEC data

Jewel E. Thomas[*1], Ubong C. Ben[2], Ndifreke I. Udosen[1], Ekong U. Nathaniel[1]

Received: April 8, 2024 /Accepted: June 5, 2024

Abstract

Seismo-ionospheric abnormalities are typically detected using total electron content (TEC) measurements taken from satellites. In this study, global positioning system (GPS) - TEC data from 3 sites in the seismic zone of the magnitude 7.8 Turkey earthquake (EQ) of February 6, 2023, were examined with the ultimate aim of detecting their possible link with the impending seismic event, to mitigate loss of lives and property. For the purpose of finding abnormal and differential TEC, a statistical approach was applied to daily TEC ten days pre- and ten days post the seismic event. The results showed that the investigation period days 1, 4, 8, and 9 showed enhancement in diurnal TEC, and that KABR and CSAR sites were the only sites that registered aberrant TEC. Results of the analysis, constrained by information from contemporaneously monitored geomagnetic indices of Kernnifzer digit (kp), disturbance storm time (Dst), and solar indices (sunspot number (SSN) and F10.7 cm), indicated post-seismic induced anomalies related to the earthquake on the 8th and 9th days after the event. The TEC differential data were notably high four days post-event. This led to the mapping of TEC indices on February 9 and 10, 2023, above the EQ epicenter to investigate anomalous coordinated universal time (UTC) hours correlating with the earthquake. The global ionospheric map GIM-TEC did not link the occurrence of anomalous ionospheric clouds over the epicenter to the seismic event. This work revealed post-seismo-ionospheric variations through GPS-TEC data concomitant to the M7.8 Turkey geo-quake of February 6, 2023, which served as a short-term earthquake indicator that may have mitigated the catastrophic loss of lives and properties from its numerous aftershocks. The perturbations on the 8th and 9th days post-event served as precursors to the M6.4 February 20th earthquake.

✉ Jewel E.Thomas: jewelemem@gmail.com; jewelthomas@aksu.edu.ng

[1] Geophysics Research Group, Physics Department, Akwa Ibom State University, Nigeria

[2] Department of Physics, University of Calabar, Nigeria.

Keywords: Turkey, Earthquake, Perturbations, Ionospheric, GPS - TEC

1.0 Introduction

A catastrophic earthquake with magnitude (M) 7.8 on the Richter scale struck Southern Turkey at about 01:17:34 UTC on February 6, 2023 with its epicenter (37.225^{o}N; 37.014^{o}E) and focal depth (10 km) in the province of Kahram-anmaras, Pazarck District. Approximately nine hours after the occurrence of this earthquake (10:24:49 UTC), another major earthquake with M7.5 struck the region of Ekinozu (38.024^{o}N; 37.203^{o}E), located 90 km from the previous epicenter, resulting in calamitous damages. Approximately 9,136 aftershocks were reported, with the magnitude of some aftershocks ranging as high as 6.4 (on February 20, 2023) and 5.6 (on 27 February 2023), leading to the destruction of previously injured infrastructure. By March 13, 2023, an estimate of approximately 48,000 fatalities and 115,000 injured persons had been recorded. In addition, 2.2 million people, inclusive of refugees, had to be evacuated from the disaster zones. World Bank disaster assessment reports estimated an economic loss of more than $34 billion (USGS, 2023).

Different geological and non - geological approaches have been employed in earthquake prediction studies. Past studies have investigated induced ionospheric disorder, erratic electrical appliance behavior, variations in daily records of total electron content (TEC), and increment of radon gas content in the soil, among others (Ikeya, 2004; Akhoondzadeh, 2010; Thomas *et al*., 2019, Thomas *et al*., 2020a, b; Thomas *et al*., 2021), in a bid to forecast EQ occurrence. Evaluation of global positioning system - total electron content data has indicated a correlation between EQ and ionospheric precursors. However, due to the dearth of comprehensive evaluations of activities preceding the earthquake, activities occurring during the earthquake, and activities occurring subsequent to the earthquake within seismogenic zones, submissions of EQ forecasting from these abnormalities have been disputed. According to some researchers (Geller *et al*., 1997; Rishbeth, 2007), EQ forecasting was not feasible via methodologies used in the delineation of earthquake precursors. Nevertheless, novel statistical analyses of the Global Positioning System-TEC and satellite data (Li and Parrot, 2012), indicated that correlations existed between seismic events and the occurrence of ionospheric perturbations. In addition, previous works (Akpan *et al*., 2019; Thomas, 2020; Thomas *et al*., 2023) presented using statistical methods, the probability of earthquake occurrence via analysis of ionospheric perturbations generated from DEMETER data within seismogenic zones. Researches have been vast in pre - seismo-ionospheric perturbations (Oikonomou *et al.*, 2020; Eshkuvatov *et al*., 2023; Vesnin *et al*., 2023). Oikonomou *et al.* (2020) investigated pre-earthquake ionospheric and atmospheric disturbances for three large earthquakes in Mexico. From their reports, large and short scale ionospheric anomalies relating to the events were observed few hours to few days before the events. Also, Eshkuvatov *et al*. (2023) reported on the morphological characteristics of anomalous variations in Global Navigation Satellite System Total Electron Content (GNSS-TEC)

prior to the strong local earthquakes (EQ) that occurred during the period of 2011–2015. Vesnin *et al*. (2023) made a pioneer report on ionospheric response to the 6 February 2023 Turkey - Syria earthquake and showed significant asymmetry in the propagation of coseismic ionospheric disturbances. In all the aforementioned cases and more, emphasis is on pre-event days. It is pertinent to note that the state of the ionosphere after the EQ has received little or no attention. However, monitoring its state could provide insightful data about the numerous aftershocks that further wrecked the already destroyed properties and lives.

The aim of this research, therefore, was to evaluate pre - and post-earthquake indicators, with the objective of predicting their occurrence to aid in the mitigation of colossal losses of lives and property. This research was necessitated by the backdrop of the humongous death toll and material damage recorded in this earthquake and other such physical cataclysms. This work, therefore, aimed at delineating ionospheric perturbations obtained simultaneously at three GPS stations in the preparatory zone of the Turkey EQ. The goal was to identify probable seismogenic alterations that were the likely source of the observed Turkey EQ of February 6, 2023 and its numerous aftershocks. In this wise, an equal duration before and after the seismic event was adopted in this research.

2.0 Earthquake Data

To assess TEC within the seismogenic area, seismo-ionospheric disturbances associated with the M7.8 Turkey EQ were examined using data obtained from three GPS sites. Figure 1 gives the Geographical location of M7.8 Turkey EQ in relation to the three GPS stations, while Table 1 displays their coordinates and distances to the epicenter.

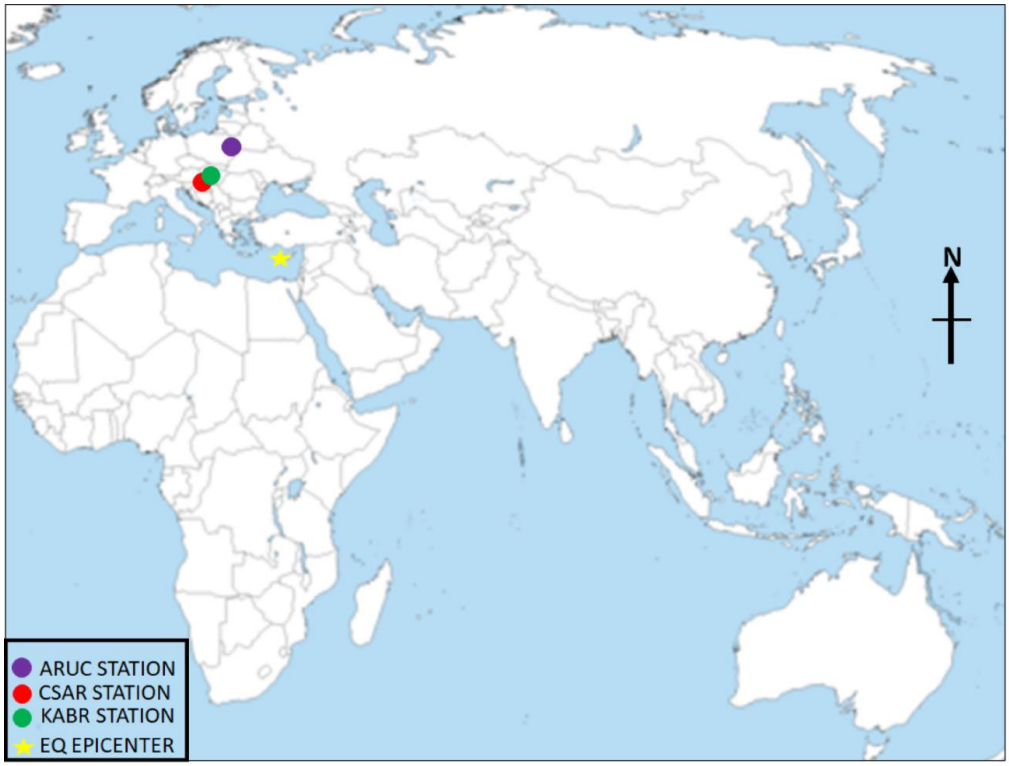

Figure 1: Geographical location of M7.8 Turkey EQ. The yellow star denoted the EQ epicenter; the purple, red, and green circles denoted the three GPS locations (ARUC, CSAR and KABR sites, respectively) located within the seismogenic zone.

Table 1: GPS stations geographical coordinates and distance from epicenter

Location	Geographical Latitudes (N^0)	Geographical Longitudes (E^0)	Distance from Epicenter (km)
Epicenter	37.225	37.014	-
KABR	33.023	35.145	497
CSAR	32.488	34.890	561
ARUC	40.286	44.086	701

Data acquired from the sun-spot number (SSN), the 10.7cm microwave flux density (F10.7cm solar flux), the geomagnetic indices (planetary geomagnetic activity kp and disturbance storm time Dst), and the TEC were employed to scrutinize pre- and post-seismic ionospheric variations. The SSN and F10.7cm solar-flux information filtered influences from solar activities, whereas data from kp and Dst measured the impact of geomagnetic activity. The Space Physics Environment Data Analysis Software (SPEDAS) provided SSN, F10.7 cm solar flux, equator-ward geomagnetic activity index (Dst) and planetary geomagnetic activity index (kp) data.

The 10.7cm microwave flux density, represented by F10.7 solar flux, was a crucial component in determining solar activity. The F10.7cm solar flux was related to solar activity, which was quantified using the SSN. The F10.7 cm magnitude ranged from 60 to 300 Solar Flux Units (SFU). SFU < 100 was considered quiet. Using Dst data with an hourly temporal resolution, geomagnetic activities in middle and low latitude zones were identified. Minor magnetic storms were indicated by values ranging from 50 nT<Dst ≤ -30 nT; medium magnetic storms were indicated by -100nT<Dst ≤ -50nT; large magnetic storms were indicated by -200nT <Dst ≤ -100nT; and severe magnetic storms were indicated by Dst ≤ -200nT (Xinzhi *et al*., 2014).

Employing a three-hourly time resolution, the kp index identified global geomagnetic actions, which ranged from 0 (low activity) to 9 (high action), with a kp index < 3 indicating a decline in geomagnetic activity (Rostoker 1972). Carrier phase data were used to estimate the comparative total electron contents and quantitative ambiguities, and pseudo ranges were used to estimate uncertainty integers and absolute TECs. The global ionosphere map (GIM), which had a spatial resolution of 2.5 degrees (latitude) and 5 degrees (longitude) and a temporal resolution of two hours, was received from the International Global Navigation Satellite System (GNSS) Service Community (ftp://cddis.gsfc.nasa.gov/-pub/gps/products/ionex).

3.0 Method

Diurnal GPS-TEC data from three stations located in the preparatory regions of the geo-quake was retrieved to identify temporary anomalies. TEC data generated 10 days prior to the EQ and 10 days subsequent to the EQ were employed. The boundaries employed for the data were the standard deviation and the confidence interval of the mean as given in equations 1 and 2:

$$x_u = \mu + 2\sigma \quad (1)$$

$$x_l = \mu - 2\sigma \quad (2)$$

where x_u= the upper limit, x_l = the lower limit, μ = the mean quantity and σ = the standard deviation. These bounds, μ and σ were determined during the course of the investigation. TEC values outside these limits were regarded as abnormal. A similar method was used by Thomas *et al*. (2023). The geomagnetic and solar indices within the study period were analyzed. In addition, the daily TEC maps defined with two-hourly temporal resolutions above the EQ geographical point for the 3rd and 4th days (9th and 10th February, 2023) post-event were acquired from GIM-TEC for the examination of spatial anomalies.

Equations 3 and 4 indicate the TEC differential values as follows:

$$x_l < x < x_u \rightarrow -2 < \left(\frac{x-\mu}{\sigma}\right) < 2 \quad (3)$$

and

$$D_x = \left(\frac{x-\mu}{\sigma}\right) \quad (4)$$

where x_u= upper limit, x_l= lower limit, x = the parametric quantity, μ = mean quantity, σ = standard deviation, and D_x = differential of x. Given $|D_x| \geq 2$, the behavior of x would be deemed abnormal. EQ anomalies were evaluated in this study via TEC data obtained at the three GPS sites in Turkey. The preparation area (in kilometers) for the M7.8 Turkey seismic event was evaluated via the empirical formula of Dobrovolsky *et al.* (1979) in equation 5:

$$R = 10^{0.43M} \quad (5)$$

where R = radius of the EQ preparatory zone, and M = EQ magnitude. A value of 2,259.436 km was therefore obtained as the preparatory zone for the M7.8 Turkey seismic events of February 6, 2023. Equation 5 indicated that the size of the preparatory zone was a function of EQ magnitude, and vice versa. To choose atypical data for this study, stringent criteria were employed: $|\Delta TEC| \geq 2.0$; $Dst < -30nT$; $Kp > 3$; $F10.7 < 100SFU$ (Thomas *et al.*, 2024).

4.0 Results

Results obtained were indicated on 2D graphs delineated in Figures 2 (a-c) and 3. Figure 2 illustrates the top and bottom panels within each site. The ordinate indicated TEC information (top panel) and the differential of TEC (bottom panel), while the abscissa indicated the pre- and post-seismic event days, with black vertical lines denoting the seismic day (February 6th, 2023). On the top panel of each plot (see Figure 2), the daily TEC values, the upper boundaries x_u, and the lower boundaries x_l were denoted by blue, red, and green wiggles, respectively. The lower panel illustrates the daily TEC differential values (dTEC) generated from equation (4), with black spikes denoting anomalous values. Figure 2a denoted the KABR site, Figure 2b denoted the CSAR site, and Figure 2c denoted the ARUC site. The lower panels of Figure 2 clearly showed post-seismic perturbations within the investigative period. In order to confirm variations within 10 days pre-event and 10 days post-event, within normal limits, ionospheric anomalies above the epicenter in Turkey were studied using GPS-TEC.

Figure 3a illustrates plots of the geomagnetic indices Dst, figure 3b illustrated plot of kp, Figure 3c illustrated plots of SSN, and Figure 3d illustrates plots of F10.7cm, all within the investigative period. The EQ Day was denoted by black vertical lines. The ordinate indicated the values of the different parameters, while the abscissa indicated the number of days relative to the EQ.

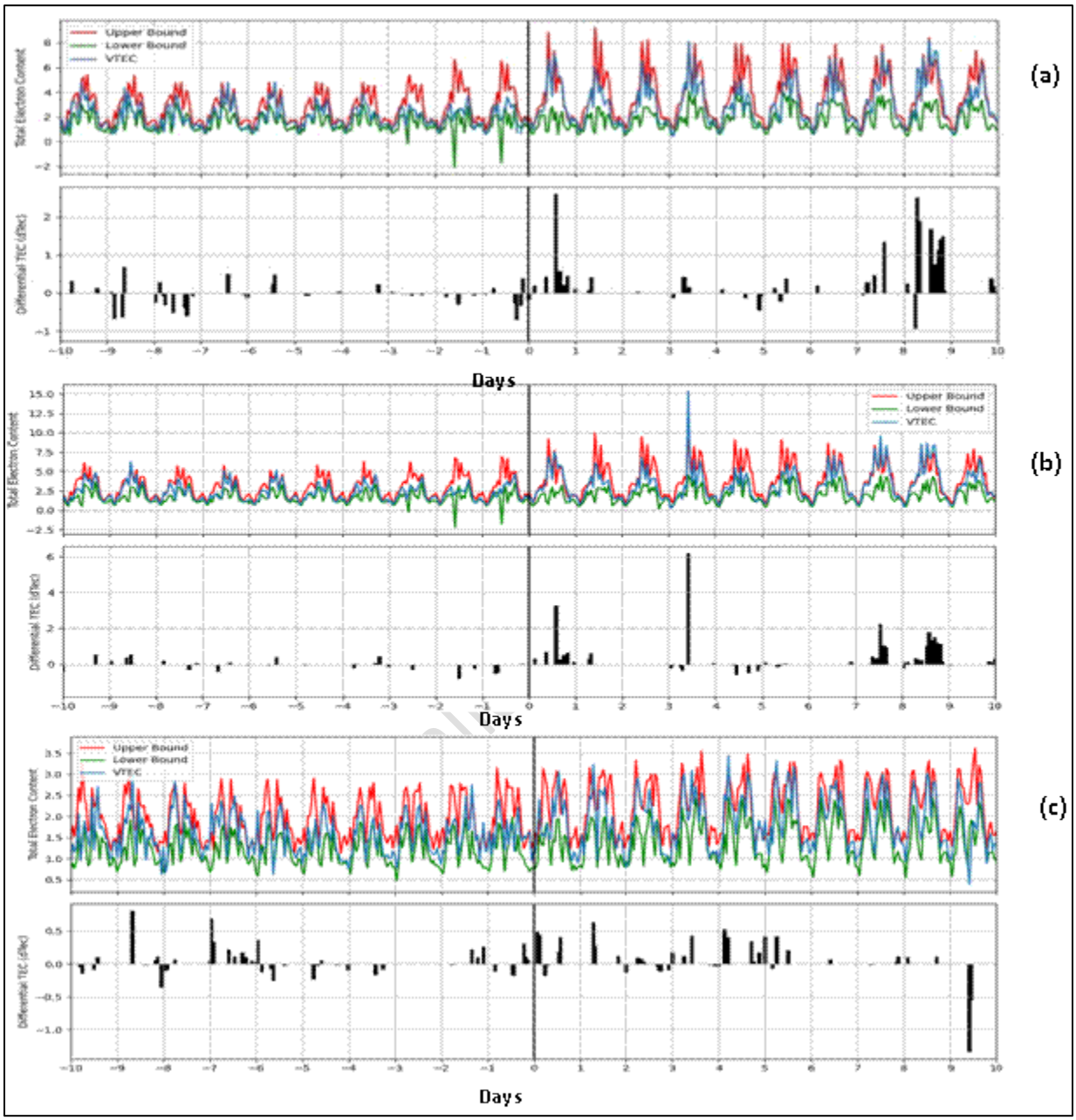

Figure 2 (a – c): The diurnal Global Positioning System-TEC measurements before and after the M 7.8 Turkey seismic event of February 6, 2023, within the confidence ranges. Figure (a) denoted the KABR site, (b) denotes the CSAR site, and (c) denotes the ARUC site. The investigative window spanned January 27 through February 16, 2023.TEC was measured in 10^{16}el/m^2. The number of days pre- and post-event was plotted as abscissa and Total Electron Content was plotted as ordinate. The main-shock was denoted by a black vertical line.

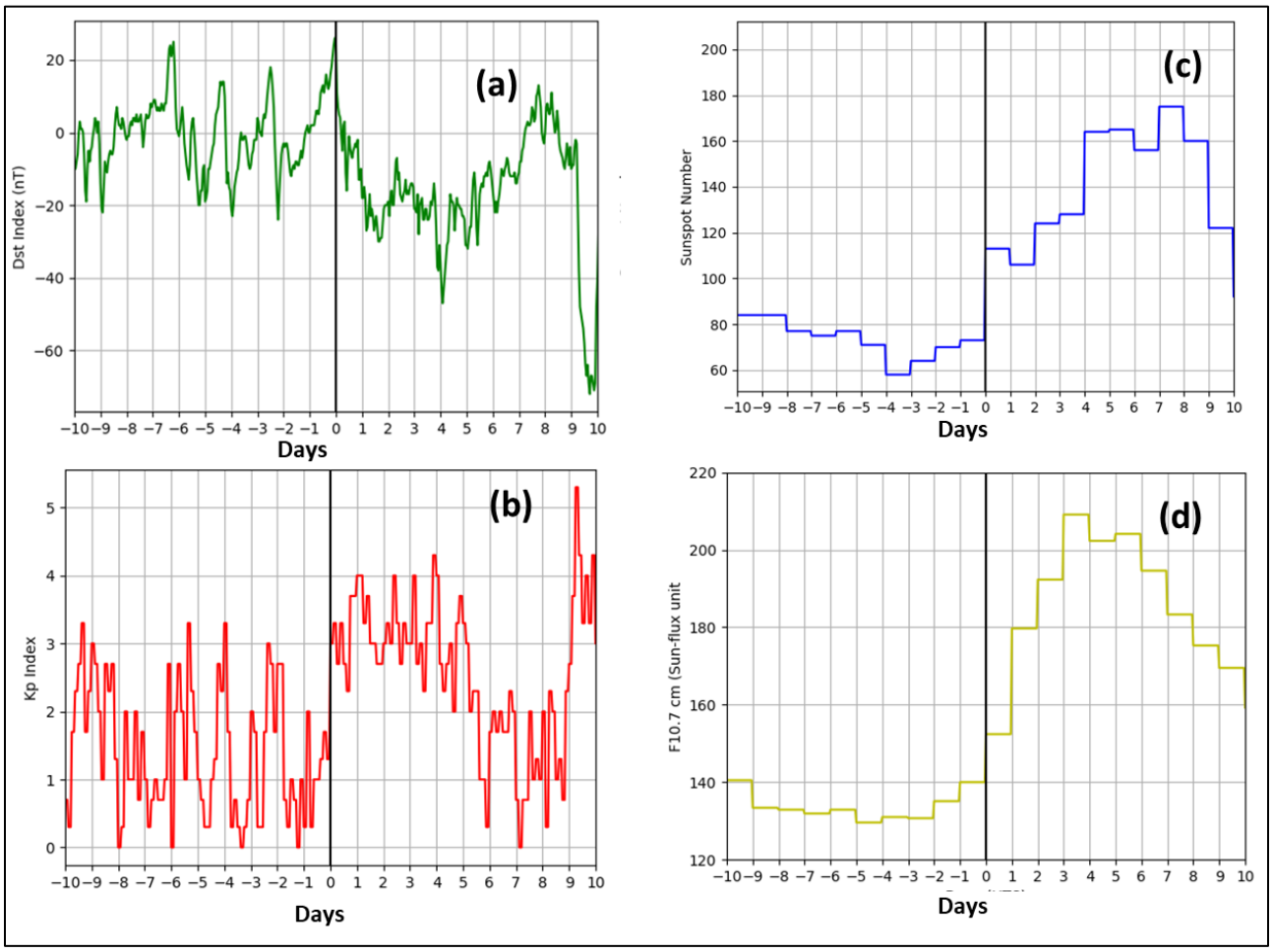

Figure 3: Geomagnetic and solar activity (January 27 - February 16, 2023): (**a**) Disturbance storm time index (**b**) kp index (**c**) Sunspot number SSN (**d**) F10.7cm index

5.0 Discussion

Figure 2 indicated striking anomalies from daily TEC values in two of the GPS stations that were outside the confidence bounds. All observed variations that met the stringent conditions for selecting the anomalous days were recorded after the EQ Day (post-seismic) from the two GPS stations. These two stations KABR and CSAR (Figure 2a and 2b) were closer to the epicenter while the farthest ARUC station (Figure 2c) had no abnormal TEC from the stringent set of criteria employed. This observation is different from the reports of Thomas *et al*. (2023) in which all three stations recorded anomalies. From the KABR GPS station which was the closest to the epicenter (Table1), post-event days 1 and 9 displayed anomalous disturbances, while at the CSAR GPS station, post-event days 1, 4 and 8 revealed anomalous TEC information. From these results, post-event day one was simultaneously disturbed at two GPS stations. Constraining these results by contemporaneously monitored geomagnetic and solar indices revealed that post-event days 1 and 4 were active as seen in Figure 3. The kp and Dst indices were >3.0 and < -30nT on these two days. Anomalously high $|\Delta TEC|$ were measured four days after the seismic event (Figure 2b). Hence,

space maps of TEC (Figure 4) generated for February 9th and 10th, 2023 (i.e., the 3rd and 4th days post-event) above the epicenter of Turkey M7.8 EQ were employed to investigate if such anomalous TEC values correlated with the Coordinated Universal Time (UTC) hours of the EQ. In-depth analysis of these GIM-TEC maps (Figure 4) indicated that the anomalous ionospheric clouds were unrelated to the impending EQ. This, however, was different from the results of Thomas *et al.* (2022), where the unusual clouds observed were related to the M7.2 Haiti EQ of August 14, 2021.

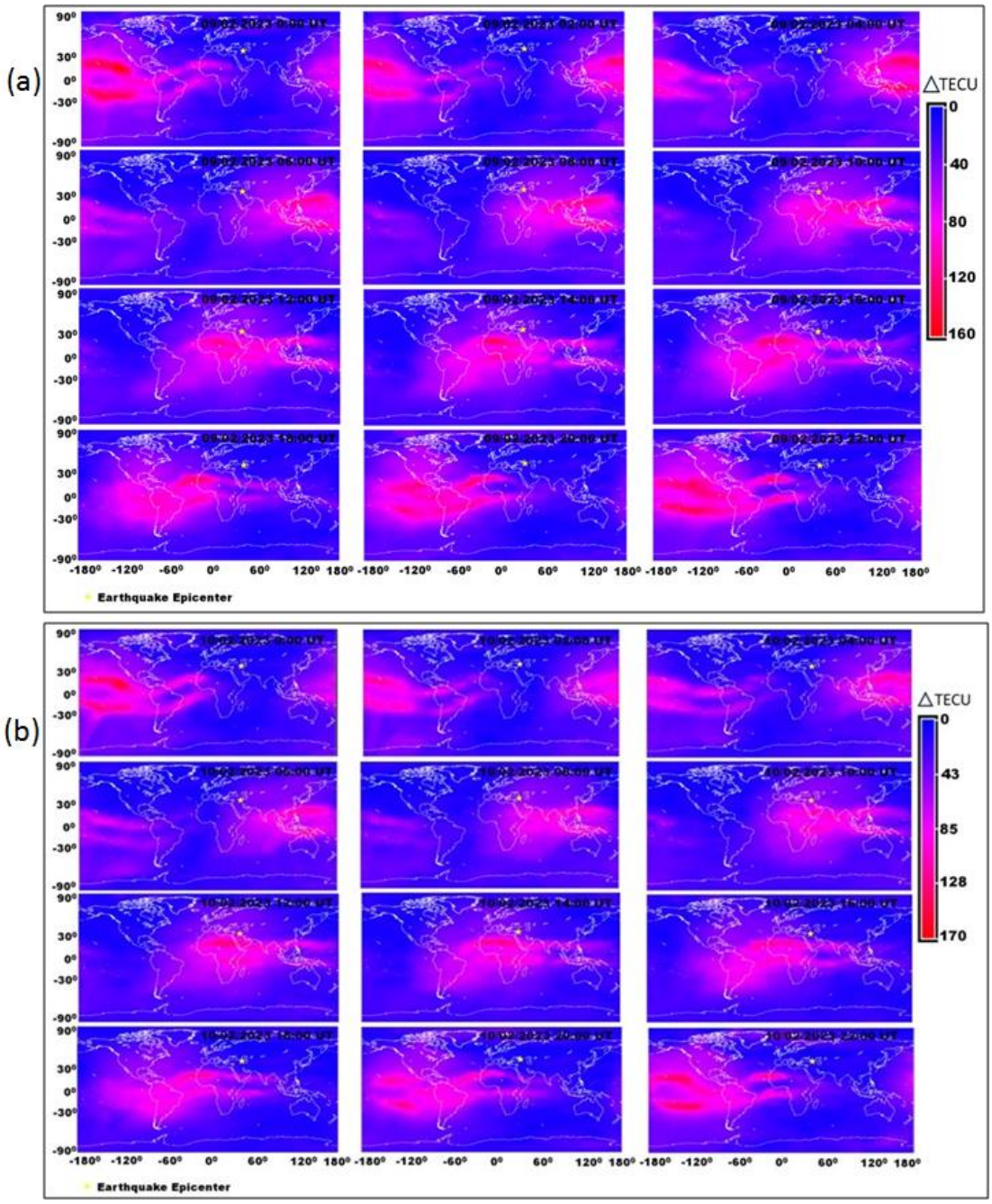

Figure 4: Spatial TEC maps above the epicenter of the M7.8 Turkey seismic event: (**a**) February 9th, 2023, (**b**) February 10th, 2023. The yellow star on Figures (4a) and (4b) indicate the epicentral position of the geo-quake; the legend indicates the TECU (TEC unit) within each Universal Time hour.

Correlating the perturbations of 8- and 9-days post-event (February 14 and 15) with geomagnetic and solar indices indicated that these perturbations occurred during quiet conditions. These two days actually occurred 5 and 6 days before the aftershock on February 20th. This work has therefore given valuable evidence that noticeable ionospheric anomalous activity was detected after the M7.8 Turkey EQ of February 6, 2023, which served as precursors to the M6.4 aftershock of February 20, 2023. The results obtained correlate with past research that indicated that ionospheric perturbations are detected days prior to, during and after major seismic events (e.g., Liu *et al*., 2004, Ibanga *et al*., 2018; Thomas, 2021; Thomas *et al*., 2023). Such seismic-induced electric field from below may be related to either reduction or augmentation in the ionosphere.

6.0 Conclusion

Total Electron Content data from three GPS sites located within a seismogenic domain was used to evaluate seismo-ionospheric abnormalities connected to the M7.8 Turkey EQ of February 6, 2023.The study recorded no pre-ionospheric response within the investigative period from the three GPS stations used. However, two out of the three stations indicated positive post- EQ anomalous values in TEC. The results indicated that these two stations namely KABR and CSAR stations presented unusual variations on post event days 1, 4, 8, and 9. These results showed strong seismically generated perturbations on days 8 and 9, unlike those on days 1 and 4 which were aseismic from concurrently monitored solar and geomagnetic indices. $|\Delta TEC|$ was observed to be significantly high on 4 days post-event, hence, spatial maps from TEC data on February 9th and 10th, 2023 (3 and 4 post-event days), across the epicenter of the magnitude 7.8 earthquake was screened to indicate if the Coordinated Universal Time hours correlated with the seismic event. No remarkable unusual clouds in the ionosphere were revealed through GIM - TEC data as relating to the seismic event. This research has therefore identified significant post-seismic ionospheric abnormalities linked to Turkey's M7.8 earthquake on February 6, 2023, using GPS-TEC data. These post-seismic variations formed possible precursors (-5 and -6 days) to the M6.4 aftershock of February 20, 2023.

Acknowledgements

The IGS community's contribution to the GIM-TEC data is appreciated by the authors. Furthermore, we express our thanks to the United States Geological Survey as well as SPEDAS for contributing data on earthquakes, geomagnetic storms, and solar activity.

References

Akhoondzadeh, M., Parrot, M. and Saradjian, M.R. (2010). Electron and ion density variations before strong earthquakes (M> 6.0) using DEMETER and GPS data. Natural Hazards and Earth System Sciences, 10(1), pp.7-18. https://doi.org/-10.-5194/nhess-10-7-2010

Akpan, A.E., Ibanga, J.I., George, N.J. and Ekanem, A.M., (2019): Assessing seismo-ionospheric disturbances using Vanuatu and Honshu earthquakes of March 25, 2007, employing DEMETER and GPS data.

International journal of environmental science and technology, 16, pp.7187-7196.https://doi.org/10.1007/s13762-019-02339-x

Dobrovolsky, I.P., Zubkov, S.I. and Miachkin, V.I., (1979): Estimation of the size of earthquake preparation zones. Pure and applied geophysics, 117(5), pp.1025-1044. https://doi.org-/10.1007/bf00876083

Eshkuvatov, H.E. Ahmedov, B.J.,Tillayev, Y.A., Arslan Tariq, M. Ali Shah, M., Libo Liu,(2023). Ionospheric precursors of strong earthquakes observed using six GNSS stations data during continuous five years (2011–2015), Geodesy and Geodynamics, 14, (1), 65-79, 1674-9847, https://doi.org/10.1016/j.geog.2022.04.002.

Geller, R.J., Jackson, D.D., Kagan, Y.Y. and Mulargia, F., (1997): Earthquakes cannot be predicted. Science, 275(5306), pp.1616-1616.https://doi.org/10.1126/science.275.5306.1616

Ibanga, J. I., Akpan, A. E., George, N. J., Ekanem, A. M. and George, A. M. (2017). Unusual ionospheric variations before the strong Auckland Islands, New Zealand earthquake NRIAG; *J. Astron. Geophys.* **7(1)** 149–154, https://doi.org/ 10.1016-/j.nrjag.2017.12.007.

Ikeya, M., (2004): Earthquakes and animals: From folk legends to science. World Scientific. Singapore. https://doi.org/10.11-42/5382

Li, M. and Parrot, M., (2012): "Real time analysis" of the ion density measured by the satellite DEMETER in relation with the seismic activity. Natural hazards and earth system sciences, 12(9), pp.2957-2963. https://doi.org/10.5194/nhess-12-2957-2012

Liu, J.Y., Chuo, Y.J., Shan, S.J., Tsai, Y.B., Chen, Y.I., Pulinets, S.A. and Yu, S.B., 2004, April. Pre-earthquake ionospheric anomalies registered by continuous GPS TEC measurements. In Annales geophysicae (Vol. 22, No. 5, pp. 1585-1593). Göttingen, Germany: Copernicus Publications. https://doi.org/10.5194/angeo-22-1585-2004

Oikonomou, C., Haralambous, H., Pulinets, S., Khadka, A., Paudel, S. R., Barta, V. and İnyurt, S. (2020). Investigation of pre-earthquake ionospheric and atmospheric disturbances for three large earthquakes in Mexico. *Geosciences*, *11*(1), 16.

Rishbeth, H., (2007): Do earthquake precursors really exist? Eos, Transactions American Geophysical Union, 88(29), pp.296-296. https://doi.org/10.1029/2007eo290008

Rostoker, G., (1972): Geomagnetic indices. Reviews of Geophysics, 10(4), pp. 935-950. https://doi.org/10.1029/rg010i00-4p00935

Thomas, J.E., George, N.J., Ekanem, A.M. and Ekpenyong, N.E., (2019): Ionospheric induced plasma disturbances afore the M7. 9 eastern Sichuan China earthquake of 12th May, 2008.International Journal of Advanced Geosciences. https://doi.org/10.-14419/ijag.v7i2.29980

Thomas, J.E., George, N.J., Ekanem, A.M. and Nathaniel, E.U., (2020a): Preliminary investigation of earth tremors using total electron content: a case study in parts of

Nigeria. NRIAG Journal of Astronomy and Geophysics, 9(1), pp.220-225. https://doi.-org/10.1080/20909977.2020.1723866

Thomas, J.E., George, N.J., Ekanem, A.M. and Akpan, A.E., (2020b): Ionospheric plasma variations afore the east of Kuril Islands earthquake of 13th January, 2007. Geological Behavior, 4(1), pp.42-46. https://doi.org/10.26480/gbr.01.2020.42.46

Thomas, J.E., Ekanem, A.M., George, N.J. and Akpan, A.E., (2021): Electron temperature and ion density perturbations prior to the M 6.8 Eastern Honshu, Japan earthquake of July 23, 2008. Journal of Earth System Science, 130(3), p.134. https://doi.org-/10.1007/s12040-021-01645-8

Thomas, J.E., Ekanem, A.M., George, N.J. and Akpan, A.E., (2023): Ionospheric perturbations: a case study of 2007 five major earthquakes using DEMETER data. Acta Geophysica, 71(4), pp.1607-1618. https://doi.org/10.1007/s11600-023-01059-8

Thomas, J. E, Ben, U. C. Ekanem, A. M. George, N. J., Nathaniel, E. U. (2022)**:** Seismo-ionospheric anomalies before M7.2 Haiti earthquake of August 14, 2021, from GPS-TEC, Acta Geophysica. https://doi.org/10.-1007/s1160 0-022-00903-7

Thomas, J. E. (2021): Lithosphere-atmosphere - Ionosphere coupling fog Pre-, Co- and post-earthquakes: a case study of Northern Mariana, USA earthquake of 31st October 2007. Res J Sci Technol 1(1):37–46

Thomas, J.E. (2020): SEISMO–Ionospheric Induced Perturbations Prior to the September 28, 2007 M7. 5 Northern Mariana USA Geoquake from GPS, TEC and DEMETER Data, Journal of Geosciences (MJG) 4 (1), 38-42

Thomas, J E; Nathaniel, E U; George, N J; Ekanem, A M and Akpan, S S (2024). Statistical analysis of detected ionospheric anomalies with earthquake magnitudes: A case study of the New Zealand earthquakes of March 4, 2021 Results in Earth Sciences 2, 100011

Vesnin, A., Yasyukevich, Y., Perevalova, N. and Senturk, E. (2023): Ionospheric Response to the 6 February 2023 Turkey–Syria Earthquake. Remote sensing 15(9), 2336; (https://doi.org/10.3390/rs15092336)

Xinzhi, W., Junhui, J., Dongjie, Y. and Fuyang, K. (2014): Analysis of ionospheric VTEC disturbances before and after the Yutian Ms7. 3 earthquakes in the Xinjiang Uygur Autonomous Region. Geodesy and Geodynamics, 5(3), pp.8-15.https://doi.org/10.3724/sp.j.1246.2014.03008